Inhibition of Aluminium Corrosion in 1M HCl by Pyridoxine Hydrochloride: Thermodynamic and Quantum Chemical Studies

**Mamadou Yeo[1], Mougo André Tigori[2*], Amadou Kouyaté[2],
Paulin Marius Niamien[1] and Albert Trokourey[1]**

[1]*Laboratoire de Constitution et de Réaction de la Matière, Université Félix Houphouët-Boigny, 22 BP 582 Abidjan 22, Côte d'Ivoire.*
[2]*UFR Environnement, Université Jean Lorougnon Guédé, BP 150 Daloa, Côte d'Ivoire.*

Authors' contributions

This work was carried out in collaboration among all authors. Author MY designed the study, performed the statistical analysis, wrote the protocol and wrote the first draft of the manuscript. Authors MAT and AK managed the literature searches and the analyses of the study. Authors PMN and AT supervised the work and instructed all the research. All authors read and approved the final manuscript.

Original Research Article

ABSTRACT

Currently, research in the area of corrosion inhibition is focussed on the development of green corrosion inhibitors. It is with this in mind that pyridoxine hydrochloride, which is vitamin B6, has been tested as a corrosion inhibitor of aluminium in 1M HCl by mass loss, Density Functional Theory (DFT) and Quantitative Structure-Property Relationship (QSPR) methods. The results obtained show that the inhibition efficiency increases with concentration but decreases with increasing temperature. This vitamin is adsorbed on aluminium according to the modified Langmuir isotherm and occurs in two modes: physisorption and chemisorption. Thermodynamic adsorption and activation parameters have been determined and discussed. Finally, QSPR approach was used to find the best set of parameters in order to determine the theoretical inhibition efficiencies from the experimental data. Experimental measurements were found in good collaboration with the theoretical results.

_____

Corresponding author: E-mail: tigori20@yahoo.fr;

1. INTRODUCTION

The use of light metals in the automotive industry and other sectors has become a solution for saving fuel [1] and reducing greenhouse gases. Among light metals, aluminium is the most widely used because of its many outstanding properties. This massive use of aluminium exposes it to the corrosion phenomenon. Corrosion is a chemical or electrochemical reaction with all kinds of materials (metals, ceramics, polymers etc.) in variable environments (aqueous atmosphere, high temperatures etc.) and leads to a degradation of the material and its properties. Indeed, during its use, aluminium is covered with oxide or scale and to remove this oxide, the metal part is immersed in an appropriate acid solution, called an acid pickling bath. The acid solution attacks and dissolves the scale or part of the metal, which eventually renders the metal part unusable [2].

The current trend to reduce this phenomenon is the use of eco-friendly organic corrosion inhibitors [3-8]. Applications of these inhibitors play a major role in environmental protection because they are less toxic and biodegradable [9-12]. They have heteroatoms and π bonds that would facilitate their adsorption on the metal surface [13-15]. Vitamin B6 or pyridoxine hydrochloride (Fig. 1) has been used as a corrosion inhibitor in this work because it contains heteroatoms (oxygen and nitrogen) that can facilitate its adsorption on the aluminium surface and it is eco-friendly and non-toxic.

Moreover, the adsorption process of an organic inhibitor on the metal surface is explained by kinetic and thermodynamic parameters are useful tools. These parameters permit to specify whether the adsorption process is endothermic or exothermic and to indicate the nature of this adsorption [15-19].

The advent of chemical calculations using density functional theory (DFT) at B3LYP/6-31G (d) level allows to calculate the electronic parameters of a molecular system with a very high degree of accuracy [20-23]. These parameters are then used to estimate the binding tendency of various inhibitory molecules on the metal surface, thus the inhibition efficiency. In addition, quantitative structure-property relationship (QSPR) method is used to correlate the experimental inhibition efficiency with the inhibition properties of the molecule studied in 1M hydrochloric acid solution. According to some authors [24-27], QSPR concept can be used to relate the inhibition efficiency of most organic inhibitors to their structural parameters.

The objective of the present study is to evaluate, on the one hand, the kinetic parameters of aluminium dissolution and the thermodynamic parameters of pyridoxine hydrochloride or adsorption on the aluminium surface and, on the other hand, to establish a relationship between the chemical parameters of the studied compound and the experimental inhibition efficiency.
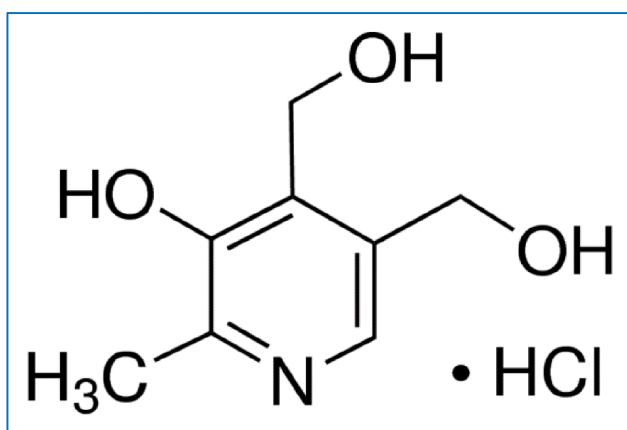
Fig. 1. Molecular structure of pyridoxine hydrochloride (PHC)

2. MATERIALS AND METHODS

2.1 Materials

Hydrochloric acid solution with purity 37% and acetone with purity 99.5% used in this work were purchased from MERCK. Analytical grade pyridoxine hydrochloride (Fig. 1) purchased from SIGMA ALDRICH was used to prepare solutions of concentrations range from 0.13 to 0.53 mM. Aluminium samples of 99.5% purity were in the form of a rod measuring 10 mm in length and 2 mm in diameter. A precision balance from STARTORIUS was used to weigh the samples. The samples were dried in a proofer from MEMMERT. The temperature was controlled by a thermostat water bath from MEMMERT.

2.2 Mass Loss Measurements

These samples were successively polished with metallographic emery paper having an increasing fineness of different grains (40, 80, 240 and 600) and cleaned with acetone, washed with double distilled water and dried in a proofer. After being weighed, the samples were introduced into the 1M hydrochloric acid solution test in the absence or presence of different concentrations of pyridoxine hydrochloride which are 0.13mM, 0.18mM, 0.27mM and 0.53mM. In order to evaluate corrosion as a function of temperature, a water thermostat was used to control and maintain the temperature in the range of 298K to 323K. After one hour of immersion, sufficient time to evaluate the inhibitor performance, the samples were removed from the solution, washed with a bristle brush under double distilled water to remove corrosion product, dried and weighed. The tests were performed in aerated solutions and were carried out in triplicate to ensure reliable results. Indeed, this technique, which allows the effective study of mass loss, is in line with other corrosion monitoring techniques such as electrochemical methods and surface analysis techniques.

The mass loss obtained permit to calculate the corrosion rates (W), the degree of surface coverage (θ) and the inhibition efficiency IE (%) using the following expressions:

$$W = \frac{\Delta m}{S_e . t} = \frac{m_1 - m_2}{S_e . t} \tag{1}$$

$$\theta = \frac{W_0 - W}{W_0} \tag{2}$$

$$IE(\%) = \frac{W_0 - W}{W_0} * 100 \tag{3}$$

Δm: is the mass loss (g) m_1 and m_2 are respectively, the weight (g) before and after immersion in the solution test; t: the immersion time (h) ; S_e : the total surface of sample (cm^2) ; w_0 and w : are respectively the corrosion rates of aluminium in the absence and presence of pyridoxine hydrochloride.

2.3 Theory and Computational Details

2.3.1 Density Functional Theory (DFT) method

Density functional theory (DFT) is an application incorporated in the commercial software (Gaussian). Quantum chemical calculations were carried out by Gaussian 03 software [28]. These theoretical calculations were used to find the relationship between the molecular structure of pyridoxine hydrochloride and its inhibition efficiencies. This application has permitted to optimize the geometry of the studied compounds (Fig. 2) at B3LYP level, with 6-31G(d) basis set [29,30].
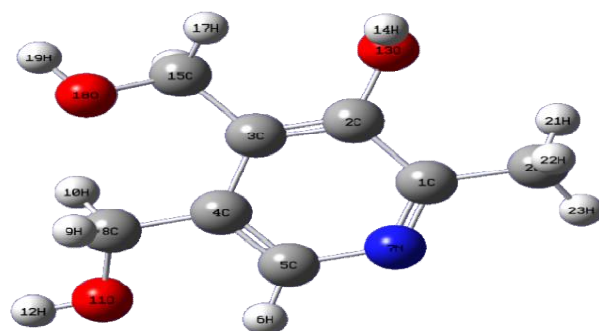
Fig. 2. Optimized structure of pyridoxine hydrochloride with B3LYP/6-31G (d)

The corresponding quantum chemical parameters including the global parameters such as the highest occupied molecular orbital energy (E_{HOMO}), the lowest unoccupied molecular orbital energy (E_{LUMO}), energy gap (ΔE), dipole moment (μ), the electron affinity (A), the ionization energy (I) ,the electronegativity (χ), the hardness (η), the softness (σ), the electrophylicity index (ω), the fraction of electron transferred (ΔN) , total energy (E_T). Local parameters such as Fukui function f_k^+ or f_k^- and dual descriptor (Δf_k^+ or Δf_k^-) will be useful to predict the reactivity sites [31]. These parameters can be calculated according to the following expressions [32-34]:

$$\Delta E = E_{LUMO} - E_{HOMO} \tag{4}$$

$$I = -E_{HOMO} \tag{5}$$

$$A = -E_{LUMO} \tag{6}$$

$$\chi = -\mu_p = \left(\frac{\partial E}{\partial N}\right)_{v(r)} \tag{7}$$

$$\chi = \frac{I+A}{2} \tag{8}$$

$$\eta = \frac{I-A}{2} \tag{9}$$

$$\sigma = \frac{1}{\eta} = \frac{2}{I-A} \tag{10}$$

$$\omega = \frac{\mu_P^2}{2\eta} = \frac{(I+A)^2}{4(I-A)} \tag{11}$$

$$\Delta N = \frac{\phi_{Al} - \chi_i}{2(\eta_{Al} + \eta_i)} \tag{12}$$

Where ϕ_{Al} = 4.28 eV and the hardness of aluminium η_{Al} = 0 [35], χ_i and denote the electronegativity and the η_{inh} hardness of the inhibitor molecule.

Fukui function measures local reactivity. This function is considered as the first derivative of electronic density $\rho(r)$ with respect to the number of electrons N at a constant external v(r) [36]. Using a scheme of finite difference approximations, this procedure condenses the values around each atomic site into a single value that characterizes the atom in the molecule the values around each atomic site into a single value that characterizes the atom in the molecule [37,38].

$$f_k = \left[\frac{\partial \rho(r)}{\partial N}\right]_{v(r)} \tag{13}$$

$$f_k^+ = [q_k(N+1) - q_k(N)] \text{(For nucleophilic attack)} \tag{14}$$

$$f_k^- = [q_k(N) - q_k(N-1)] \text{(For electrophilic attack)} \tag{15}$$

Where $q_k(N+1)$, $q_k(N)$ and $q_k(N-1)$ are the electronic population of atom k in $(N+1)$, N and $(N-1)$ electrons systems.

The dual descriptor recently introduced by some authors [39,40] allows to efficiently locate the probable sites of nucleophilic and electrophilic attack. The condensed form of the dual descriptor can be computed using the following equation:

$$\Delta f_k(r) = f_k^+ - f_k^- \tag{16}$$

If $\Delta f_k(r) > 0$,the process is driven by a nucleophilic attack, and the atom k acts as an electrophile, for $\Delta f_k(r) < 0$ the process is driven by an electrophilic attack and the atom k acts as a nucleophile.

2.3.2 Quantitative Structure-Property Relationship (QSPR) method

QSPR has also been used to correlate the experimental inhibition efficiency with quantum chemical parameters. This approach provides mathematical relationships that indicate correlations between some sets of descriptors and the corrosion performance of a molecule and provides clear direction on the selection of new inhibitors to guide research [41]. We will apply the non-linear multivariate model proposed by Lukovits et al to study the interactions between corrosion inhibitors and metal surfaces in 1M HCl. This model [42] is represented by the relation:

$$IE_{calc}(\%) = \frac{[Ax_j + B]C_i}{1 + [Ax_j + B]C_i} * 100 \tag{17}$$

In this case, C_i represents the different concentrations for the inhibitor, which are $130\mu M$, $180\mu M$, $270\mu M$ and $530\mu M$,A and B are real constants which will be determined when solving the system of equations. We tested sets of three parameters (x_1, x_2, x_3). Then the equation becoming:

$$IE_{calc}(\%) = \frac{[Ax_1 + Bx_2 + Dx_3 + E]C_i}{1 + [Ax_1 + Bx_2 + Dx_3 + E]C_i} * 100 \tag{18}$$

This equation allows us to have a system of four equations with four unknowns A, B, D and E. It is thus a question of finding for the molecule the set

of coefficients A, B, D and E which permits to obtain the value of the inhibition efficiency closest to the experimental value. The calculations were carried out using the EXCEL software.

3. RESULTS AND DISCUSSION

3.1 Effect of Temperature and Inhibitor Concentration on the Corrosion Process

Fig 3 gives the effect concentration and temperature on corrosion rate of aluminium.

Fig. 3 shows clearly that the corrosion rate of aluminium increases with temperature, but decreases with increasing inhibitor concentration. This indicates that the addition of pyridoxine hydrochloride in the corrosive medium HCl 1M delays the corrosion of aluminum even if the presence of chloride ions favors the corrosion trend on the metal surface. Indeed the inhibitor acts as a physical barrier between the aluminium and the corrosive medium, this barrier is more reinforced when the inhibitor concentration increases. Similar results have been found in the literature [43,44].

The evolution of inhibition efficiency as a function of temperature for different concentrations is shown in Fig. 4.
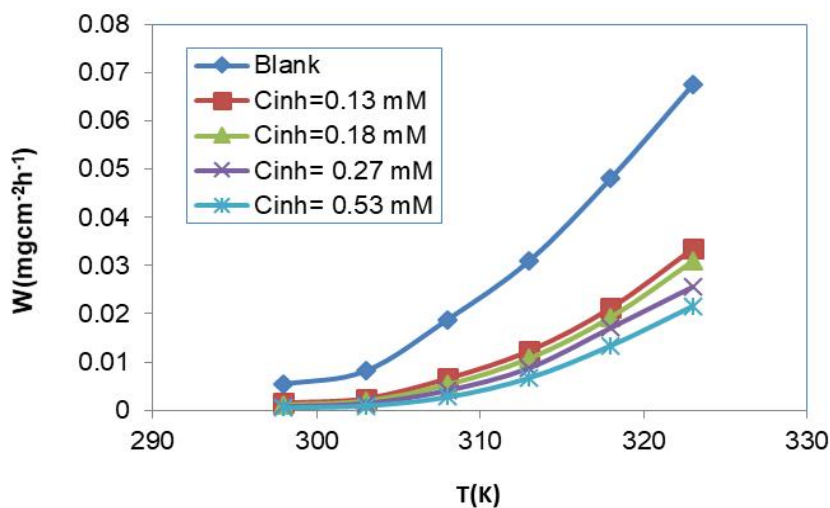
Fig. 3. Variation of corrosion rate as a function of temperatures at different concentrations
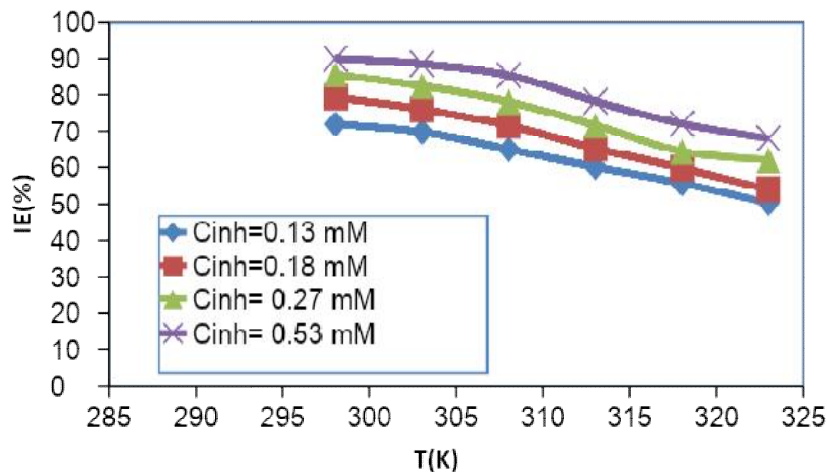
Fig. 4. Inhibition efficiency versus temperatures for different concentrations

Inspection of the Fig. 4 reveals that the inhibition efficiency of pyridoxine hydrochloride decreases with increasing temperature and increases with concentration. We observe for Cinh= 0.53mM: IE(%)= 90,56 at 298K and IE(%)= 73,86 at 323K.Moreover this observation can also be explained by the increased solubility of the protective film that includes the inhibitor and corrosion products initially precipitated on the metal surface [45], which progressively exposes the metal surface to the attacks of the aggressive medium as the temperature increases.

3.2 Effect of Immersion Time on Inhibition Efficiency

In order to study the inhibition efficiency of pyridoxine as time changes, the aluminium samples were immersed in hydrochloric acid solutions of concentration 1M, with and without addition of pyridoxine hydrochloride of concentration 0.53mM at the temperature of 298K for immersion times which are 30min, 60min, 90min, 120 min, 150min, 180 min, 210min, 240 min and 270min. Fig. 5 shows the evolution of inhibition efficiency as a function of immersion time.

The results obtained show that the inhibition efficiency decreases progressively with increasing immersion time and tends to stabilize between 180min and 270min, which is consistent

with those found in previous studies for shorter durations [46]. These results reveal that pyridoxine hydrochloride creates in the first instance a strong barrier by giving electrons to the aluminium to isolate it from the corrosive environment. This barrier progressively decreases before stabilizing to ensure minimal protection of the metal. We can therefore deduce that for long immersion times, the adsorbed inhibitor molecules desorb little.

3.3 Adsorption Isotherm

Adsorption isotherms provide valuable basic information on the interaction between the inhibitor and the metal surface as well as the adsorption mechanism which depends on the electronic characteristics of the inhibitor, the metal nature, the surface and the temperature. The general form [47] of these isotherms is given by the relationship:

$$f(\theta,x)\, exp\, exp\, (-g\theta) \;=\; K_{ads}C_{inh} \qquad (19)$$

Where, $f(\theta,x)$ is the configurational factor subject to the physical model and assumptions involved in the derivation of the isotherms, C_{inh} is the inhibitor concentration, θ is the surface coverage, K_{ads} is the equilibrium constant of the adsorption process and g is a parameter that expresses the interaction of the molecules in the adsorbed layer.
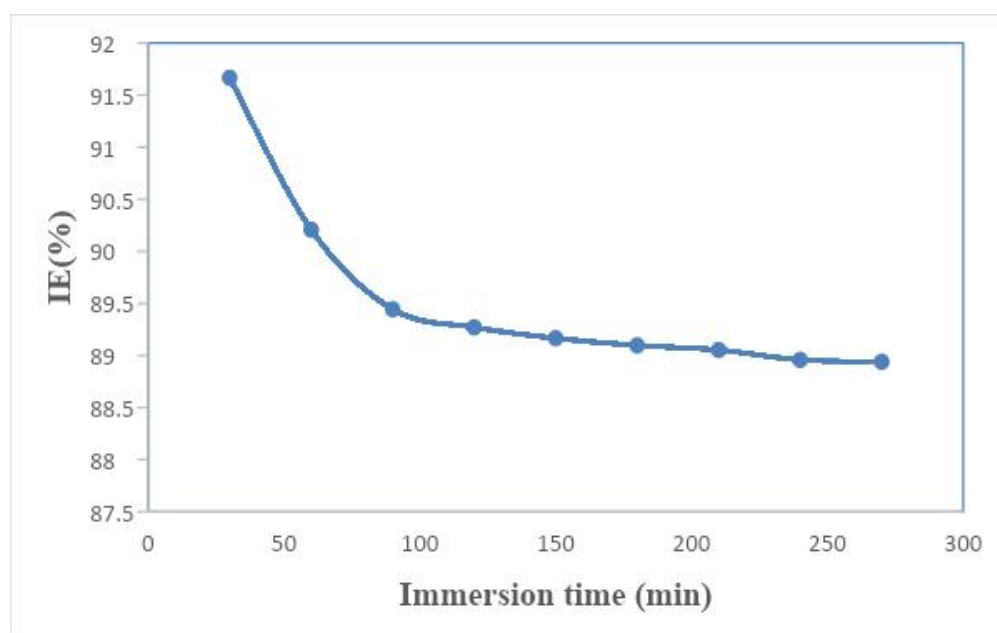
Fig. 5. Inhibition efficiency as a function of immersion time

Experimental data have been applied on different adsorption isotherms (Langmuir, El-Awady and Flory-Huggins) whose different equations are as follows

Langmuir isotherm: $\frac{C_{inh}}{\theta} = \frac{1}{K_{ads}} + C_{inh}$ (20)

El-Awady isotherm: $log\left(\frac{\theta}{1-\theta}\right) = logK_{ads} + ylogC_{inh}$ (21)

Flory-Huggins isotherm: $log\left(\frac{C_{inh}}{\theta}\right) = logK_{ads} + xlog(1 - \theta)$ (22)

Figs. 6, 7 and 8 present the study of these models.

The different parameters of the straight lines are listed in Table 1.
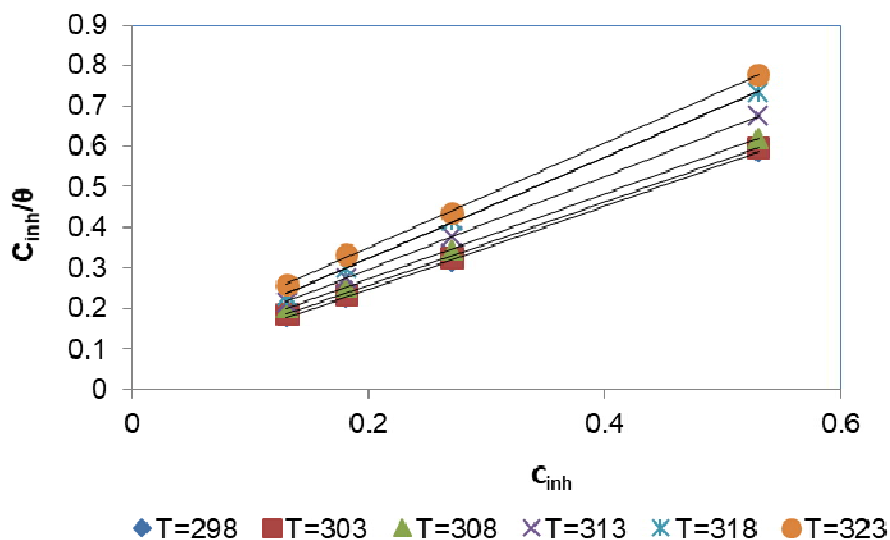
Fig. 6. Langmuir adsorption isotherm for the investigated molecule at different temperatures
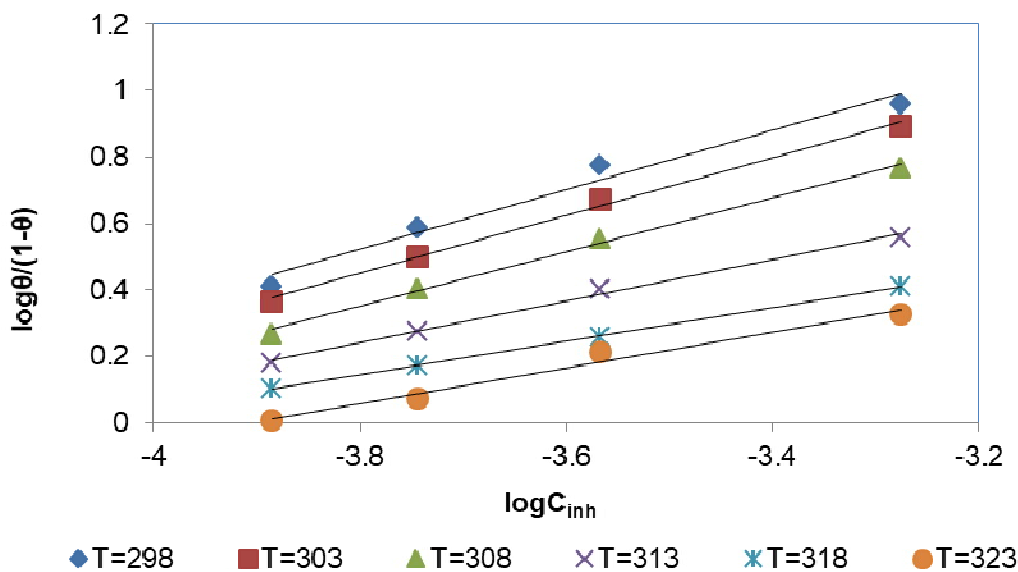
Fig. 7. El-Awady adsorption isotherm for the investigated molecule at different temperatures
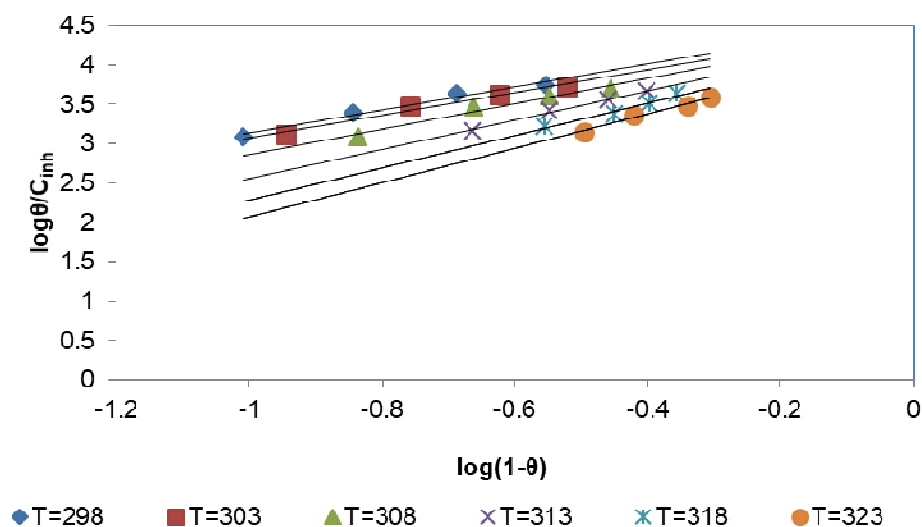
Fig. 8. Flory-Huggins adsorption isotherm for the investigated molecule at different temperatures

Table 1. Isotherms parameters for various temperatures

Isotherm	T(K)	R^2	slope	Intercept
Langmuir	298	0.9996	1.0235	0.0434
	303	0.9999	1.0303	0.0509
	308	1.0000	1.0522	0.0622
	313	1.0000	1.1494	0.0672
	318	0.9995	1.2486	0.0752
	323	0.9993	1.2951	0.0915
El-Awady	298	0.9968	0.5677	2.9972
	303	0.9994	0.4688	2.5021
	308	0.9884	0.4318	2.2342
	313	0.9943	0.3947	1.9970
	318	0.9839	0.4089	1.9667
	323	0.9916	0.4213	1.9431
Flory-Huggins	298	0.9718	1.4601	4.5987
	303	0.9691	1.4512	4.5208
	308	0.9732	1.6035	4.4659
	313	0.9937	1.8596	4.4187
	318	0.9739	2.0467	4.3370
	323	0.9780	2.1766	4.2442

A careful analysis of Table 1 clearly shows that the Langmuir isotherm has correlation coefficients closer to unity. Therefore, this adsorption isotherm proved to be the best description of the inhibitor studied. Langmuir adsorption model assumes the existence of a fixed number of energetically identical sites on the surface. Each site can adsorb only one particle. Whereas El-Awady isotherm study shows that each pyridoxine hydrochloride molecule occupies more than one active site because 1/y>1 or y is the slope of each line

obtained. The slopes of the straight lines obtained with Langmuir isotherm are greater than one, which reveals the presence of interactions between the adsorbate species on the metal surface as well as changes in the heat of adsorption with increasing coverage [48]. Although having the correlation coefficients closer to unity this isotherm cannot be strictly applied. The adsorption of pyridoxine hydrochloride can be more appropriately represented by the modified Langmuir equation or Villamil isotherm [48]

$$\frac{C_{inh}}{\theta} = \frac{n}{K_{ads}} + nC_{inh} \qquad (23)$$

3.4 Thermodynamic Adsorption Parameters

The adsorption constant (K_{ads}) determined from the modified Langmuir isotherm equation allows to calculate the variation of the standard free energy of adsorption (ΔG_{ads}^0) [50] through the following equation:

$$\Delta G_{ads}^0 = -RTln(55,5 \, K_{ads}) \qquad (24)$$

Where T is the absolute temperature, R is the perfect gas constant and 55.5 is the concentration of water in solution [51] expressed in mol. L^{-1}.

The adsorption enthalpy ΔH_{ads}^0 and adsorption entropy ΔS_{ads}^0, were also calculated using the following equation:

$$\Delta G_{ads}^0 = \Delta H_{ads}^0 - T\Delta S_{ads}^0 \qquad (25)$$

$-\Delta S_{ads}^0$ and ΔH_{ads}^0 are respectively the slope and the intercept of the straight line obtained when representing ΔG_{ads}^0 in function of the temperature (Fig. 9).

The values of $K_{ads}, \Delta G_{ads}^0, \Delta H_{ads}^0 \text{ and } \Delta S_{ads}^0$ are listed in Table 2.

Generally values of ΔG_{ads}^0 around -20 kJ.mol^{-1} or higher are consistent with physisorption while values more negative than -40 kJ.mol^{-1} are related to chemisorption [52,53]. The negative values of ΔH_{ads}^0 indicate that the adsorption of the inhibitor is an exothermic process implies two adsorption modes; chemisorption and physorption while the positive sign of ΔS_{ads}^0 reflects that the disorder increases probably due to desorption of water molecules [54].

In order to distinguish between physisorption and chemisorption, experimental data were fitted to Adejo – Ekwenchi isotherm [55] which is described by the following equation:

$$log\left(\frac{1}{1-\theta}\right) = logK_{AE} + blogC_{inh} \qquad (26)$$

Where C_{inh} is the concentration of the adsorbate, K_{AE} and b are the isotherm parameters. Fig. 10 gives the plots of $log\left(\frac{1}{1-\theta}\right)$ versus $logC_{inh}$.

$\Delta G = -0.038T - 23.38$
$R^2 = 0.98$
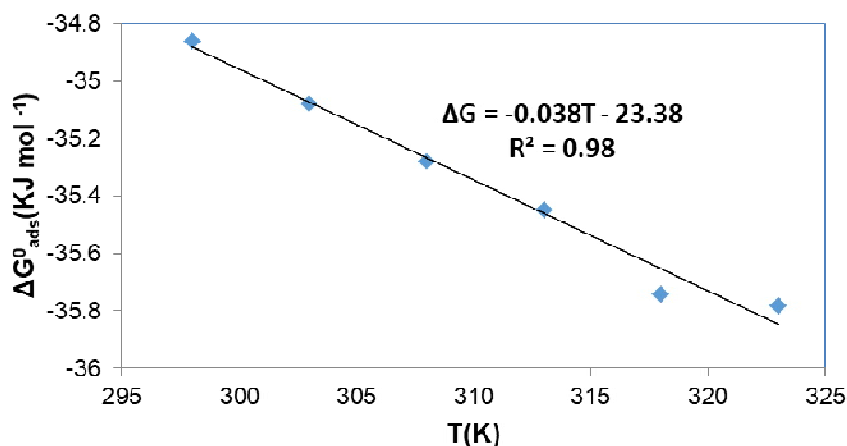
Fig. 9. Variation of ΔG_{ads}^0 as a function of temperature

Table 2. Thermodynamic parameters of PHC adsorption on aluminium in 1M HCl

T (K)	K_{ads}(M^{-1})	ΔG_{ads}^0 (KJ. mol^{-1})	ΔH_{ads}° (kJ.mol^{-1})	ΔS_{ads}^0(J. mol^{-1}. K^{-1})
298	23041	-34.9	−23.38	38.00
303	19646	-35.1		
308	16077	-35.3		
313	14881	-35.4		
318	13298	-35.7		
323	10929	-35.8		
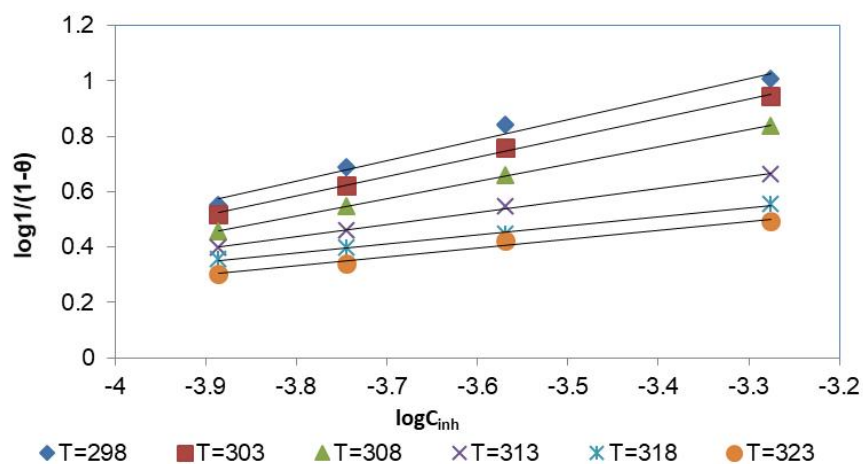
Fig. 10. Adejo – Ekwenchi isotherm for PHC adsorption on aluminium in 1M HCl

Table 3. Adejo – Ekwenchi isotherm parameters

T(K)	R^2	b	K_{AE}
298	0.9823	0.7414	3.4562
303	0.9983	0.699	3.2413
308	0.9996	0.6241	2.884
313	0.9823	0.4361	2.0925
318	0.9969	0.3280	1.6261
323	0.9829	0.3216	1.5539

The parameters of the straight lines are gathered in in Table 3.

Analysing the Table 3 shows that parameter b decreases from 298K to 313K, indicating the physisorption in this temperature range. From 318K to 323K, the parameter b is practically constant and shows that the adsorption of pyridoxine hydrochloride occurs chemically (chemisorption) [56]. We can conclude that the molecule studied adsorbs on aluminum according to two adsorption modes: physisorption and chemisorption with predominance of physisorption. Finally, we note that physisorption is carried out at relatively low temperatures, contrary to chemisorption, which is carried out at high temperatures.

3.5 Activation Parameters

The activation energy of the aluminium dissolution reaction can be determined by the Arrhenius relation:

$$W = A.exp\left(-\frac{E_a}{R.T}\right) \qquad (27)$$

Where W is the corrosion rate in the presence of inhibitor, E_a the apparent activation energy of the corrosion process, R the universal gas constant,

A is the frequency factor, T is the absolute temperature. Fig. 11 gives the representation of $\log W$ as a function of the inverse of temperature.

The slope $(-\frac{E_a}{2,3.R})$ of each the straight line obtained is used to determine the activation energy.

Eyring transition state equation was used to calculate the variations of activation enthalpy ΔH_a^* and activation entropy ΔS_a^*.

$$\log(\frac{W}{T}) = \log(\frac{R}{\aleph h}) + \frac{\Delta S_a^*}{2,303R} - \frac{\Delta H_a^*}{2,303RT} \qquad (28)$$

Where h the Planck constant, $\aleph$ the Avogadro number.

Indeed, the representation of $\log(\frac{W}{T})$ as a function of 1/T for different pyridoxine hydrochloride concentrations (Fig. 12) gives straight lines whose slopes are $-\frac{\Delta H_a^*}{2,303R}$ and the intercepts $log(\frac{R}{\aleph h}) + \frac{\Delta S_a^*}{2,303R}$ allow to deduce respectively the variations of enthalpy activation (ΔH_a^*) and entropy activation (ΔS_a^*). The values of the activation parameters are recorded in the Table 4.
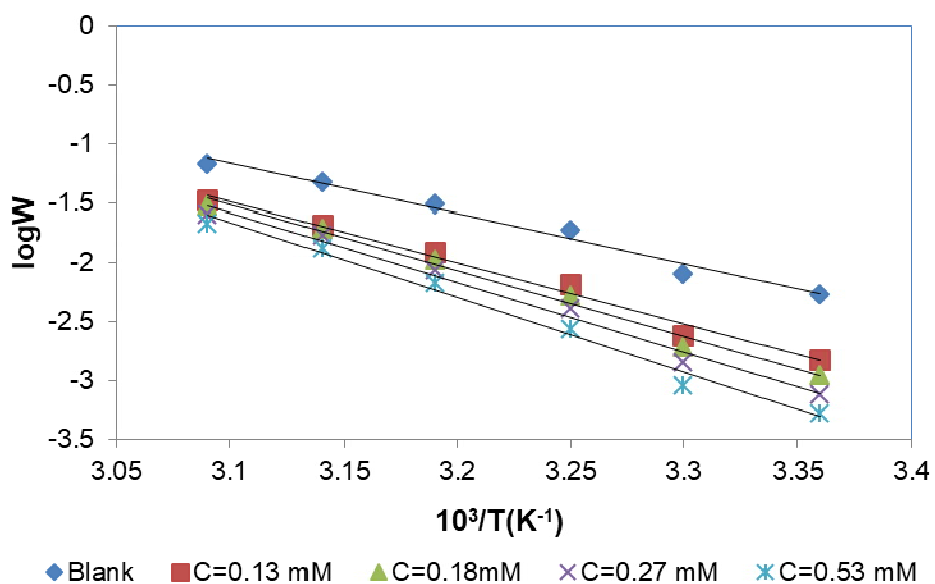
Fig. 11. Arrhenius plot for different concentrations of PHC in 1M HCl
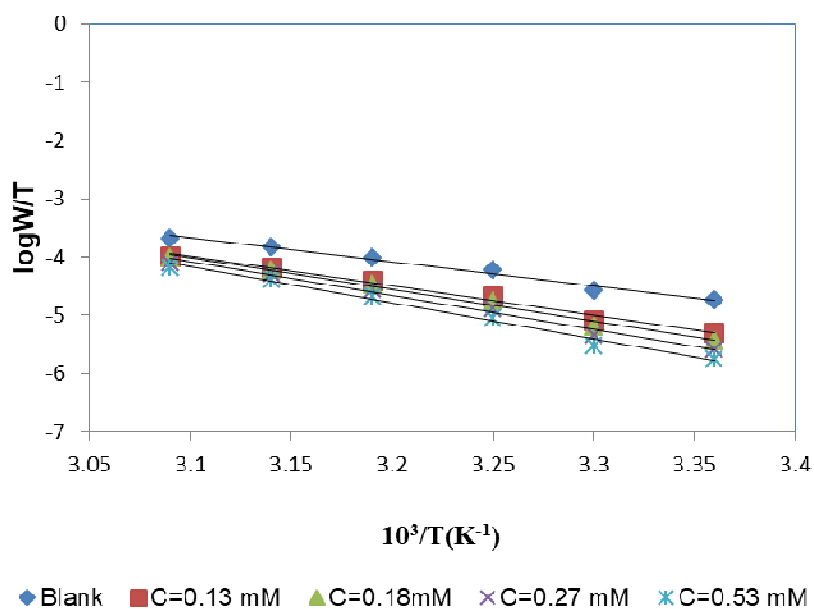
Fig. 12. Transition state plots for different concentrations of PHC in 1M HCl

Table 4. Activation parameters of aluminium in 1M HCl without and with PHC

C_{inh}(mM)	E_a $(kJmol^{-1})$	ΔH_a^*(kJ. mol^{-1})	ΔS_a^*(J.$mol^{-1}.K^{-1}$)
Blank	81.05	78.60	-24.20
0.13	99.19	96.70	26.00
0.18	106.39	103.90	47.70
0.27	113.03	110.60	67.10
0.53	120.75	118.20	89.10

The activation energy (E_a) values in the inhibited solutions are higher than that in the uninhibited solution (blank), indicating that physical adsorption is predominant [57]. Indeed physisorption, involves electrostatic forces between ionic charges or dipoles on the adsorbed species and the electric charge at the metal/solution interface .Thus the inhibitor is adsorbed on the aluminium by electrostatic bonds. These bonds are weak and sensitive to high temperature. Therefore, the inhibition efficiency of the studied molecule decreases with increasing temperature. This explains the high inhibition efficiencies obtained at low temperatures. In summary, the protection becomes weak with increasing temperature, resulting in low electronic exchanges between the inhibitor and the aluminium at high temperature. The values of the change in enthalpy of dissolution (ΔH_a^*) are positive, indicating that the dissolution of aluminium is an endothermic process [58]. These values also increase as the concentration of pyridoxine hydrochloride increases. This indicates that in its presence aluminum offers a high resistance to corrosion. The positive sign of ΔS_a^* in presence of pyridoxine hydrochloride indicates an increase in the disorder, probably due to desorption of the adsorbed species, suggesting that the activated complex is dissociation rather than an association.

3.6 Quantum Chemical Assessment

For analysing the inhibitor properties in order to describe the inhibition mechanism, density functional theory (DFT) has been used. So quantum chemical parameters chemical has been calculated by using this theory. The values are recorded in Table 5.

Table 5. Quantum Chemical parameters for PHC obtained with DFT at B3LYP/6-31G (d)

Parameters	PHC
E_{HOMO} (eV)	-6.114
E_{LUMO} (eV)	-0.648
Energy gap ΔE (eV)	5.466
Dipole moment μ (D)	2.146
Ionization energy I (eV)	6.114
Electron affinity A (eV)	0.648
Electronegativity χ (eV)	3.381
Hardness η (eV)	2.733
Softness σ (eV)$^{-1}$	0.366
Fraction of electron transferred ΔN	0.164
Electrophylicity index ω	2.091
Total energy $E_T (Ha)$	-591.86

E_{HOMO} value indicates the ability of an organic compound to donate electrons to the metal surface, high E_{HOMO} value of a compound, enhances his ability to inhibit metal corrosion, by forming an inhibitor barrier, whereas lower E_{LUMO} value indicates the molecule to be more susceptible towards accepting electrons [59]. Energy gap ($\Delta E = E_{LUMO} - E_{HOMO}$), is used to interpret the reactivity of a molecule, because a molecule with a low energy gap value is a good inhibitor [60]. The values of these indicators obtained confirm the good performance of pyridoxine hydrochloride in exchanging electrons with aluminium. The electron densities of the frontier molecular orbitals LUMO and HOMO, were presented in Fig. 13.

(a)   **(b)**

Fig. 13. (a) HOMO and (b) LUMO orbitals of PHC
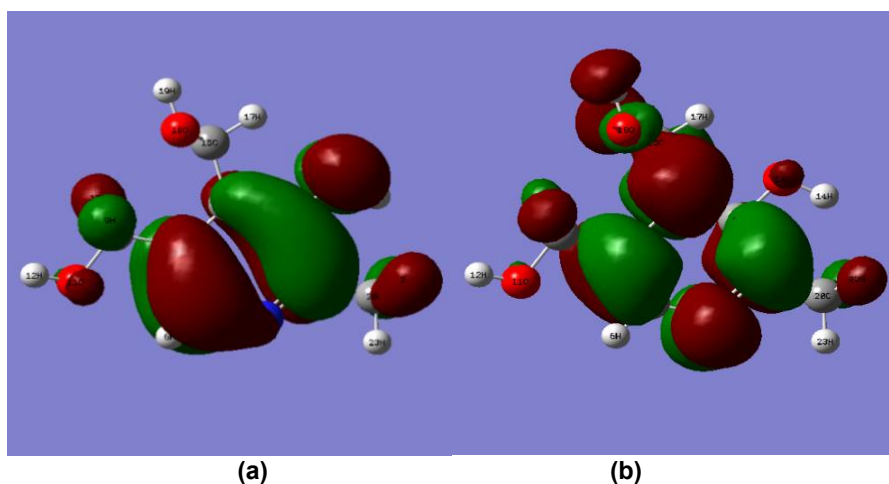
In general, according to the literature, there is no significant relationship between the value of dipole moment and the efficiency of inhibition [61,62].

Ionization energy (I) and electron affinity (A), which are respectively associated with the HOMO and LUMO energies, are fundamental descriptors of the chemical reactivity of a molecule. A high ionization energy [63] indicates that the molecule is stable and inert to any chemical reaction, while a low ionization energy indicates that the molecule is reactive. The low ionization energy of pyridoxine hydrochloride indicates his high inhibition efficiency obtained experimentally.

Hardness (η) and softness (σ) parameters are the basic chemical concepts, called global reactivity descriptors which have been theoretically justified within the framework of DFT. A hard molecule has a large energy gap and a soft molecule has a small gap [63]. Soft molecules are more reactive than hard ones because they can easily offer electrons to an appropriate acceptor. In our study the value low value of hardness (η=2.733 eV) indicates that pyridoxine hydrochloride is a soft molecule, in this case it adsorbs easily to the aluminium surface creating a protective film to reduce corrosion, which justifies the experimental results.

According to Lukovits study [42], if the value of the transferred electrons (ΔN) of an inhibitor is less than 3.6, the inhibition efficiency increases through the increase of electron-donating ability to the metal surface. In our work the fraction of electron transferred (ΔN) of pyridoxine hydrochloride is less than 3.6. This explains the capacity of pyridoxine hydrochloride to donate electrons increases its inhibition efficiency, which confirms the experimental data.

The electrophilicity index (ω) measures the propensity of chemical species to accept and give electrons [34]. The value of the electrophilic index (2.091eV) and electrons transferred ($\Delta N = 0.164$) are high, which shows that the molecule has the capacity to receive electrons. Pyridoxine hydrochloride can receive electrons from aluminium, which would enhance the adsorption of the inhibitor to the metal surface.

To better elucidate the reactivity sites, Fukui functions and dual descriptor have been investigated. These values are shown in Table 6 and have been used to locate with precision the probable sites for nucleophilic and electrophilic attacks. This localisation have given a good understanding of the interaction metal-molecule.

Table 6. Mulliken charges, Fukui functions and dual functions of PHC by B3LYP/6-31G (d)

Atom	$q_k(N-1)$	$q_k(N)$	$q_k(N+1)$	f_k^-	f_k^+	$\Delta f_k(r)$
1 C	0.236069	0.288969	0.353729	-0.0529	-0.06476	0.01186
2 C	0.219017	0.231385	0.276012	-0.012368	-0.044627	0.032259
3 C	0.051792	0.120104	0.144883	-0.068312	-0.024779	-0.043533
4 C	0.058206	0.059895	0.060096	-0.001689	-0.000201	-0.001488
5 C	-0.043764	-0.008991	0.097297	-0.034773	-0.106288	**0.071515**
6 H	0.078503	0.160543	0.244333	-0.08204	-0.08379	0.00175
7 N	-0.578174	-0.474674	-0.419302	-0.1035	-0.055372	-0.048128
8 C	-0.108619	-0.093484	-0.10225	-0.015135	0.008766	-0.023901
9 H	0.099784	0.162052	0.218154	-0.062268	-0,056102	-0,006166
10 H	0.075457	0.12849	0.193991	-0.053033	-0.065501	0.012468
11 O	-0.627053	-0.620081	-0.597586	-0.006972	-0.022495	0.015523
12 H	0.360253	0.39638	0.434592	-0.036127	-0.038212	0.002085
13 O	-0.71783	-0.657971	-0.545016	-0.059859	-0.112955	0.053096
14 H	0.393087	0.419225	0.465192	-0.026138	-0.045967	0.019829
15 C	-0.184864	-0.133109	-0.115082	-0.051755	-0.018027	-0.033728
16 H	0.096802	0.134921	0.182667	-0.038119	-0.047746	0.009627
17 H	0.068734	0.167111	0.19279	-0.098377	-0.025679	**-0.072698**
18 O	-0.618357	-0.61487	-0.610264	-0.003487	-0.004606	0.001119
19 H	0.288783	0.394261	0.429002	-0.105478	-0.034741	-0.070737
20 C	-0.495424	-0.56803	-0.585012	**0.072606**	**0.016982**	0.055624
21 H	0.133278	0.15784	0.215456	-0.024562	-0.057616	0.033054
22 H	0.109323	0.156287	0.21482	-0.046964	-0.058533	0.011569
23 H	0.104999	0.19375	0.251499	-0.088751	-0.057749	-0.031002

The most probable site for nucleophilic attacks is controlled by the atom with the highest value of f_k^+ and $\Delta f_k(r)$ while the atom with the highest value of f_k^- and the lowest value of $\Delta f_k(r)$ controls the most probable site for electrophilic attacks. An examination of the Table 6, C (20) with the highest value of f_k^+ and f_k^- is the nucleophilic and electrophilic attacks. According to the dual descriptor, C (5) and H(17) have respectively the highest and lowest of $\Delta f_k(r)$.Therefore C(5) is the nucleophilic attack centre and H (17) is the electrophilic attack centre. According to the literature [39,40] the dual descriptor is the only parameter which is able to unambiguously expose truly the nucleophilic and electrophilic regions. So, in summary C(2) and H(17) are respectively the nucleophilic and the electrophilic attacks centres.

3.7 Quantitative Structure-Property Relationship (QSPR) Consideration

In this investigation, QSPR has also been used to correlate the experimental inhibition efficiencies of the studied inhibitor and the quantum chemical parameters. We use the experimental inhibition efficiencies at 298K which are recorded in Table 7.

Table 7. Inhibition efficiencies of PHC at 298K for different concentrations

Concentration(mM)	IE(%)
0.13	72.03
0.18	79.45
0.27	85.69
0.53	90.56

The constants calculated for the sets of parameters are listed in the Table 8.

The corresponding representative plots of the correlation between calculated and experimental efficiencies of PHC for different sets of parameters are shown in Fig. 14.

Statistical indicators were used to determine the best set of parameters to correlate experimental and theoretical inhibition efficiencies. These indicators are calculated from the following equations.

The Sum of Square Errors (SSE):

$$SSE = \sum_{i=1}^{N} \left(IE_{\exp} - IE_{calc} \right)^2 \tag{29}$$

The Root Mean Square Error (RMSE):

$$RMSE = \sqrt{\frac{\sum_{i=1}^{N} \left(IE_{\exp} - IE_{calc} \right)^2}{N}} \tag{30}$$

The Mean Percent Deviation (MPD):

$$MPD = \frac{1}{N} \sum_{i=1}^{N} \left| \frac{\left(IE_{\exp} - IE_{calc} \right)}{IE_{\exp}} \right| \tag{31}$$

The different values of these statistical indicators of PHC are recorded in Table 9

Analysis of Table 9 clearly indicates that the set of parameters ($\Delta E, \mu, \sigma$) remain the most appropriate for describing pyridoxine hydrochloride behavior. In fact, for this parameter set the values for SSE, RMSE, and MPD are the lowest.

Table 8. Values of coefficients A, B, D and E for different sets of parameters

Set of parameters	A	B	D	E
$(E_{HOMO}, E_{LUMO}, \Delta E)$	-272.129	62.890	-166.389	-795.049
$(\Delta E, \mu, \sigma)$	-123.781	-88.069	489.837	686.318
$(\Delta E, \mu, \eta)$	-519.93	-2121.475	-509.504	4495.118
$(E_{HOMO}, \Delta N, \chi)$	-4.976	-326.305	-8.294	51.151

Table 9. Different values of Statistical parameters PHC

Set of parameters	R^2	SSE	RMSE	MPD
$(E_{HOMO}, E_{LUMO}, \Delta E)$	0.979	5.16	0.99	0.0116
$(\Delta E, \mu, \sigma)$	0.982	3.95	0.98	0.0115
$(\Delta E, \mu, \eta)$	0.981	6.91	1.02	0.0129
$(E_{HOMO}, \Delta N, \chi)$	0.978	17.49	1.37	0.0234

Fig. 14. Calculated versus experimental efficiencies for different set of parameters

4. CONCLUSION

Mass loss and theoretical methods shown that pyridoxine hydrochloride has a good performance in inhibiting the corrosion of aluminium in 1M HCl. The inhibition efficiencies are concentration, temperature and immersion time dependent. This inhibitor adsorb on the aluminium surface and protect it from corrosive attack. The mode of adsorption of inhibitor on the metal surface was seen to follow modified Langmuir adsorption isotherm. The thermodynamic adsorption and activation parameters obtained support both physical and chemical adsorption mechanisms. Local reactivity parameters indicate that C(2) and H(17) are the nucleophilic and electrophilic centers of attack respectively. QSPR studies reveal that $(\Delta E, \mu, \sigma)$ is the best set of parameter to correlate experimental and theoretical inhibition efficiencies. The theoretical results were consistent with the experimental data.

DISCLAIMER

The products used for this research are commonly and predominantly use products in our area of research and country. There is absolutely no conflict of interest between the authors and producers of the products because we do not intend to use these products as an avenue for any litigation but for the advancement of knowledge. Also, the research was not funded by the producing company rather it was funded by personal efforts of the authors.

ACKNOWLEDGEMENTS

COMPETING INTERESTS

Authors have declared that no competing interests exist.

REFERENCES

1. Cole GS, Sherman AM. Lightweight materials for automotive applications, Materials Characterization. 1995;35(1):37-43.

2. Zhang GA, Xu LY, Cheng YF. Investigation of erosion–corrosion of 3003 aluminum alloy in ethylene glycol–water solution by impingement jet system, Corrosion Science. 2009;51(2):283–290.
3. Singh A, Ahamad I, Quraishi MA. Piper longum extract as green corrosion inhibitor for aluminium in NaOH solution. Arabian Journal of Chemistry. 2016;9(2):S1584–S1589.
4. Abiola KJOE, Otaigbe OJ Kio. Gossipium hirsutum L. extracts as green corrosion inhibitor for aluminum in NaOH solution, Corrosion Science. 2009;51(11):1879–1881.
5. Tigori MA, Kouyaté A, Assouma Dagri AC, Kouakou V, Niamien PM. Theoretical Investigation of Two Antiabetics Drugs as Corrosion Inhibitors of Aluminium in 1.0 M HCl: Combining DFT and QSPR Calculations. American Journal of Materials Science and Engineering. 2020;8(1):6-16.
6. Bashir S, Sharma V, Kumar S, Ghelichkhah Z, Obotd IB, Kumara A. Inhibition Performances of Nicotinamide against Aluminum Corrosion in an Acidic Medium. Portugaliae Electrochimica Acta. 2020;38(1):107-123.
7. Eddy NO, Ebenso EE, Ibok UJ. Adsorption, synergistic inhibitive effect and quantum chemical studies of ampicillin (AMP) and halides for the corrosion of mild steel in H2SO4 Journal of Applied Electrochemistry. 2010,40(1):445-456.
8. Obot IB, Obi-Egbedi NO. An interesting and efficient green corrosion inhibitor for aluminium from extracts of Chlomolaena odorata L. in acidic solution. Journal of Applied Electrochemistry, 2010;40:1977–1984
9. [9] Mamadou Y, Niamien P M, Avo B E B, Trokourey A. Thiamine hydrochloride as a potential inhibitor for aluminium corrosion in 1.0 M HCl: Mass Loss and DFT Studies Journal of Computational Methods in Molecular Design. 2018;8(1):13-25.
10. Sangeetha M, Rajendran S, Sathiyabama J, Krishnaveni A. Inhibition of Corrosion of Aluminium and its Alloys by Extracts of Green Inhibitors. Portugaliae Electrochimica Acta. 2013;31(1):41–52.
11. Rosliza R. Chapter 17: Improvement of Corrosion Resistance of Aluminium Alloy by Natural Products. In Corrosion Resistance; Intech Open: London, UK; 2012.
12. ISBN 978-953-51-0467-4.
12. Xu B, Ji Y, Zhang X, Jin X, Yang W, Chen Y. Experimental and theoretical evaluation of N, N-Bis(2-pyridylmethyl)aniline as a novel corrosion inhibitor for mild steel in hydrochloric acid.Journal of the Taiwan Institute of Chemical Engineers. 2016;59:526–35.
13. Fouda AS, Gouda MM, Abd El-Rahman SI. Benzaldehyde,2-Hydroxybenzoyl Hydrazone Derivatives as Inhibitors of the Corrosion of Aluminium in Hydrochloric Acid. Chemical and pharmaceutical bulletin. 2000;48(5):636–640.
14. Okafor PC, Osabor V, Ebenso EE. Eco friendly corrosion inhibitors: Inhibitive action of ethanol extracts of Garcinia Kola for the corrosion of aluminium in acidic medium. Pigment & Resin Technology. 2007;36(5):299-305.
15. Zheludkevich ML, Yasakau KA, Poznyak SK, Ferreira MGS. Triazole and thiazole derivatives as corrosion inhibitors for AA2024 aluminium alloy. Corrosion Science. 2005;47(12):3368–3383.
16. Verma C, Lgaz H, Verma DK, Ebenso EE, Bahadur I, Quraishi MA. Molecular dynamics and Monte Carlo simulations as powerful tools for study of interfacial adsorption behavior of corrosion inhibitors in aqueous phase: A review. Journal of Molecular Liquids. 2018;26:99-120.
17. Obot IB, Obi-Egbedi NO. Fluconazole as an inhibitor for aluminium corrosion in 0.1M HCl, Colloids and Surfaces A: Physicochemical and Engineering Aspects. 2008;330(2-3):207–212
18. Umoren SA, Obot IB, Ebenso EE. Corrosion Inhibition of Aluminium Using Exudate Gum from Pachylobus edulis in the Presence of Halide Ions in HCl.E-Journal of Chemistry. 2008;5(2):355-368.
19. Aslam J, Aslam R, Irfan Hussain LI, Nagi RER, Mohammad M, Aslam A, Mehtab P, Ajab AA, Alaa AA. Inhibitory effect of 2-Nitroacridone on corrosion of low carbon steel in 1 M HCl solution: An experimental and theoretical approach Journal of Materials Research and Technology. 2020;9(3):4061-407.
20. Eddy NO, Momoh-Yahaya H, Oguzie EE. Theoretical and experimental studies on the corrosion inhibition potentials of some purines for aluminium in 0.1 M HCl. Journal of Advanced Research. 2015;6(2):203-217

21. Belghiti ME, Echih S, Dafali A, Karzazi Y, Bakasse M, Elalaoui-Elabdallaoui H, Olasunkanmi LO, Ebenso EE, Tabyaoui M. Computational simulation and statistical analysis on the relationship between corrosion inhibition efficiency and molecular structure of some hydrazine derivatives in phosphoric acid on mild steel surface, Applied Surface Science. 2019;491:707–722.

22. Elias EE, Nwankwo UUH, Onwudiwe DC, Hosten EC. Synthesis, crystal structures, quantum chemical studies and corrosion inhibition potentials of 4-(((4-ethylphenyl)imino)methyl)phenol and (E)-4-((naphthalen-2-ylimino) methyl) phenol Schiff bases, Journal of Molecular Structure. 2017;1147:252-265.

23. Bashir S, Sharma V, Singh G, Lgaz H, Salghi R, Singh A, Kumar A. Electrochemical behavior and computational analysis of phenylephrine for corrosion inhibition of aluminum in acidic medium, Metallurgical and Materials Transactions A. 2019;50:468–479

24. Arslan T, Kandemirli F, Ebenso EE, Love II, Alemu H. Quantum chemical studies on the corrosion inhibition of some sulphonamides on mild steel in acidic medium. Corrosion Science. 2009;51(1):35–47.

25. Karelson M, Lobanov VS. Quantum chemical descriptors in QSAR/QSPR studies. Chemical Reviews. 1996;96(3):1027-1043.

26. Vera L, Guzman M, Ortega-Luoni YP. QSPR study of corrosion inhibitors; imidazolines,Journal of the Chilean Chemical Society. 2006;51(4):1034-1039.

27. Cardoso SP, Hollauer E, Borges LEP, Gomes JA, da CP. QSPR prediction analysis of corrosion inhibitors in hydrochloric acid on 22%-Cr stainless steel. Journal of the Brazilian Chemical Society. 2006;17(7):1241-1249.

28. Frisch MJ, Trucks GW, Schlegel HB, Scuseria GE, Robb MA, Cheeseman JR, Montgomery JA, Jr, Vreven T, Kudin KN, Burant JC, Millam JM, Iyengar SS, Tomasi J, Barone V, Mennucci B, Cossi M, Scalmani G, Rega N, Petersson GA, Nakatsuji H, Hada M, Ehara M, Toyota K, Fukuda R, Hasegawa J, Ishida M, Nakajima T, Honda Y, Kitao O, Nakai H, Klene M, Li X, Knox JE, Hratchian HP, Cross JB, Adamo C, Jaramillo J, Gomperts R, Stratmann RE, Yazyev O, Austin AJ, Cammi R, Pomelli C, Ochterski JW, Ayala PY, Morokuma K, Voth GA, Salvador P, Dannenberg JJ, Zakrzewski VG, Dapprich S, Daniels AD, Strain MC, Farkas O, Malick DK, Rabuck AD, Raghavachari K, Foresman JB, Ortiz JV, Cui Q, Baboul AG, Clifford S, Cioslowski J, Stefanov BB, Liu G, Liashenko A, Piskorz P, Komaromi I, Martin RL, Fox DJ, Keith T, Al-Laham MA, Peng CY, Nanayakkara A, Challacombe M, Gill PMW, Johnson B, Chen W, Wong MW, Gonzalez C, Pople JA. Gaussian 03, Revision B.05, Gaussian, Inc., Pittsburgh PA; 2003.

29. Lee C, Yang W, Parr RG. Development of the Colle-Salvetti Correlation-Energy Formula into a Functional of the Electron Density. Physical Review.1988;37:785-789.

30. Becke AD. (1993) Density-Functional Thermochemistry. III. The Role of ExactExchange. Journal of Chemical Physics .1993;98:1372-1377.

31. Mendez F, Gazquez JL. Chemical Reactivity of Enolate Ions: The Local Hard and Soft Acids and Bases Principle Viewpoint.Journal of the American Chemical Society. 1994;116(20):9298-9301.

32. Koopmans T, Über T. Die Zuordnung von Wellenfunktionen und Eigenwerten zu den Einzelnen Elektronen Eines. Atoms. Physica.1934;1(1-6):104–13.

33. Parr RG, Pearson RG. Absolute hardness: companion parameter to absolute electronegativity. Journal of the American Chemical society. 1983;105(26):7512-7516.

34. Parr RG, Szentpaly LL, Liu S. Electrophilicity index Journal of the American Chemical society. 1999;121(9):1922-1924.

35. Pearson RG. Absolute Electronegativity and Hardness:application to Inorganic Chemistry, Inorganic Chemistry. 1988;27(4):734-740.

36. Lee C, Yang W, Parr RG. Local softness and chemical reactivity in the molecules CO, SCN−and H2CO. Journal of Molecular structure: Theochem. 1988;163:305-313.

37. Parr RG, Yang W. Density functional approach to the frontier-electron theory Journal of the American Chemical society. 1984;106(14):4049–4050.

38. Yang W, Mortier WJ. The use of global and local molecular parameters for the analysis of the gas-phase basicity of amines

Journal of the American Chemical society.1986;108(19):5708–5711.

39. Martínez-Araya JI. Why the dual descriptor is a more accurate local reactivity descriptor than Fukui functions? journal of Mathematical Chemistry.2015;53:451–465.

40. Morell CA, Toro-Labbé GA. New Dual Descriptor for Chemical Reactivity. Journal of Physical Chemistry. A, 2004;109(1):205–212.

41. Jian F, Jie L. Quantum chemistry study on the relationship between molecular structure and corrosion inhibition efficiency of amides. Journal of Molecular structure : Theochem . 2002;593(1–3):179-185.

42. Lukovits I, Kalman EF. Corrosion Inhibitors—Correlation between Electronic Structure and Efficiency, Corrosion (NACE). 2001;57(1):3-8.

43. Masego D, Lukman OO, et al. Some Phthalocyanine and Naphthalocyanine Derivatives as Corrosion Inhibitors for Aluminium in Acidic Medium: Experimental, Quantum Chemical Calculations, QSAR Studies and Synergistic Effect of Iodide Ions, Molecules. 2015;20(9):15701-15734.

44. Beda RHB, Koffi AA, Ehouman D, Niamien PM, Trokourey A,Theobromine as an Aluminium Corrosion Inhibitor in 1M HCL, Journal of Chemical and Pharmaceutical Research. 2019;11(12):73-91.

45. Santhini N, Jeyaraj T. The inhibition effect of [3-(4-hydroxy-3-methoxy-phenyl)-1-phenyl-propenone] on the corrosion of the aluminium in alkaline medium.Journal of Chemical and Pharmaceutical Research. 2012;4:3550-3556.

46. Fouda AS, Al Sarawy AA, Ahmed FS, El-Abbasy HM. Corrosion inhibition of aluminium 6063 usingsome pharmaceutical compounds Protection of Metals and Physical Chemistry of Surfaces. 2009;45(5):635-643.

47. [47] G. Moretti G.,Guidi F.,Grion G. Trylamine as a green iron corrosion inhibitor in 0,5M deaerated sulphuric acid. Corrosion science. 2004;46(2):387-403.

48. Langmuir I., the constitution and fundamental properties of solids and liquids, Journal of the American Chemical Society. 1916;38(11):2221–2295.

49. Villamil RFV, Corio P, Rubin JC, Agostinho SML. Effect of sodium dodecylsulfate on copper corrosion in sulfuric acid media in the absence and presence of benzotriazole, Journal of Electroanalytical Chemistry.1999;472(2):112-116.

50. Vashi RT, Champaneri VA. Toluidines as corrosion inhibitors for zinc in sulphamic acid Indian Journal of Chemical Technology. 1997;4:180-184.

51. Fils J, Zakroczmski, T. Impedance Study of Reinforcing Steel in Simulated Pore Solution with Tannin,Journal of The Electrochemical Society. 1996;143(8):2458-2464.

52. Oguzie EE, Li Y, Wang FH. Corrosion inhibition and adsorption behavior of methionine on mild steel in sulfuric acid and synergistic effect of iodide ion, Journal of Colloid and Interface Science. 2007;310(1):90-98.

53. Abboud Y, Hammouti B, Abourriche A. et al. 5-Naphthylazo-8-hydroxyquinoline (5NA8HQ) as a novel corrosion inhibitor for mild steel in hydrochloric acid solution Research on Chemical Intermediates. 2012;38:1591–1607.

54. Durnie W, Marco RD, Jefferson A, Kinsella B. Development of a Structure-Activity Relationship for Oil Field Corrosion Inhibitors. Journal of Electrochemical Society. 1999;146(5):1751-1756.

55. Adejo SO, Ekwenchi MM. IOSR. Resolution of adsorption characterisation ambiguity through the Adejo-Ekwenchi adsorption isotherm: A case study of leaf extract of Hyptis suaveolen poit as green corrosion inhibitor of corrosion of mild steel in 2 M HCl Journal of Emerging Trends in Engineering and Applied Sciences. 2014;8(5):201–205.

56. Adejo SO, Ekwenchi MM, Ahile JU, Gbertyo JA, Kaio A. Proposing a new empirical adsorption isotherm known as Adejo-Ekwenchi isotherm, Journal of Applied Chemistry. 2014;6(5):66-71.

57. Hazazi OA, Abdallah M. Prazole compounds as inhibitors for corrosion of aluminum in hydrochloric acid. International Journal of Electrochemical Science. 2013;8:8138-8152.

58. Lebrini M, Lagrenée M, Vezin H, Traisnel M, Bentiss F. Experimental and theoretical study for corrosion inhibition of mild steel in normal hydrochloric acid solution by some new macrocyclic polyether compounds. Corrosion Science. 2007;49(5):2254-2269.

59. Popova A, Christov M, Deligeorgiev T. Influence of the Molecular Structure on the Inhibitor Properties of Benzimidazole Derivatives on Mild Steel Corrosion in 1 M

Hydrochloric Acid, CORROSION. 2003;59(9):756-764.

60. Lewis DFV, Ioannides C, Parke DV. Interaction of a series of nitriles with the alcohol-inducible isoform of P450: Computer analysis of structure—activity relationships. Xenobiotica. 1994;24(5):401–408.

61. Khaled KF. (2008) Molecular Simulation, Quantum Chemical Calculations and Electrochemical Studies for Inhibition of Mild Steel by Triazoles. Electrochimica Acta. 2008;53(9):3484-3492.

62. Zhang SG, Lei W, Xia MZ, Wang FY. (2005) QSAR Study on N-Containing Corrosion Inhibitors: Quantum Chemical Approach Assisted by Topological Index,Journal of Molecular Structure: Theochem. 2005;732(1-3):173-182.

63. Chakraborty T, Gazi K, Ghosh DC. Computation of the Atomic Radii through the Conjoint Action of the Effective Nuclear Charge and the Ionization Energy. Molecular Physics. 2010;108(16):2081-2092.

Peer-review history:
The peer review history for this paper can be accessed here:
http://www.sdiarticle4.com/review-history/62778